




Article

Dynamic Properties and Energy Dissipation Study of Sandwich Viscoelastic Damper Considering Temperature Influence

Yeshou Xu ¹, Zhaodong Xu ^{1,*}, Yingqing Guo ², Xinghuai Huang ¹, Yaorong Dong ¹ and Qiangqiang Li ¹

¹ China-Pakistan Belt and Road Joint Laboratory on Smart Disaster Prevention of Major Infrastructures, School of Civil Engineering, Southeast University, Nanjing 211189, China; xuyeshou@163.com (Y.X.); huangxh@seu.edu.cn (X.H.); yaorong099@163.com (Y.D.); li_qiangqiang2018@163.com (Q.L.)

² Mechanical and Electronic Engineering School, Nanjing Forestry University, Nanjing 210037, China; gyingqing@126.com

* Correspondence: zhdxu@163.com

Abstract: Viscoelastic dampers are a kind of classical passive energy dissipation and vibration control devices which are widely utilized in engineering fields. The mechanical properties and energy dissipation capacity of the viscoelastic damper are significantly affected by ambient temperature. In this work, dynamic properties tests of the sandwich type viscoelastic damper at different environmental temperatures are carried out. The equivalent fractional Kelvin model which can characterize the mechanical behavior of the viscoelastic damper with varying frequencies and temperatures is introduced to describe the dynamic properties and energy dissipation capability of the sandwich viscoelastic damper. The self-heating phenomenon of the sandwich viscoelastic damper is studied with a numerical simulation, and the dynamic properties and energy dissipation variation of the viscoelastic damper with self-heating processes are also analyzed. The results show that the dynamic properties of the viscoelastic damper are significantly affected by temperature, excitation frequency and the internal self-generated heating.

Keywords: sandwich viscoelastic damper; dynamic properties tests; equivalent fractional kelvin model; self-heating phenomenon; temperature influence



Citation: Xu, Y.; Xu, Z.; Guo, Y.; Huang, X.; Dong, Y.; Li, Q. Dynamic Properties and Energy Dissipation Study of Sandwich Viscoelastic Damper Considering Temperature Influence. *Buildings* **2021**, *11*, 470. <https://doi.org/10.3390/buildings11100470>

Academic Editors: Tomasz Sadowski, Vitor Silva and Giuseppina Uva

Received: 6 August 2021

Accepted: 9 October 2021

Published: 13 October 2021

Publisher's Note: MDPI stays neutral with regard to jurisdictional claims in published maps and institutional affiliations.



Copyright: © 2021 by the authors. Licensee MDPI, Basel, Switzerland. This article is an open access article distributed under the terms and conditions of the Creative Commons Attribution (CC BY) license (<https://creativecommons.org/licenses/by/4.0/>).

1. Introduction

Viscoelastic dampers are a kind of representative passive energy dissipation and vibration control devices, which are widely used in aerospace, mechanical engineering, civil engineering, high precision instruments, etc. [1–6].

In seismic structural design and retrofit engineering, viscoelastic dampers are often added to structures, working together to protect the building and reduce the damage caused by earthquakes. So far, a large number of investigations on dynamic properties of viscoelastic dampers and their applications in civil engineering have been conducted [7–11]. Asano et al. [12] studied the dynamic properties of the viscoelastic damper with different materials and investigated the influence of external loading circles, displacement amplitudes and excitation frequencies on the mechanical properties of the viscoelastic damper. Shen et al. [13] conducted a dynamic experimental investigation of the viscoelastic damper considering the frequency, strain amplitude and temperature effect and used the fractional derivative for modeling the dynamic behavior of the viscoelastic damper. Mazza et al. [14] used diagonal steel braces and viscoelastic dampers to retrofit a ten-story steel frame building with and without fire damages. A combination of two Maxwell models and one Kelvin model in parallel is employed to characterize the viscoelastic behavior of the damper. The dynamic response analysis of the structure shows that the viscoelastic dampers can effectively control the vibration of the fire-damaged steel structure after retrofitting. Christopoulos et al. [15] developed a viscoelastic coupling damper for application in vibration controls for tall buildings. It has been proved that the viscoelastic coupling

damper can reliably reduce both dynamic responses caused by wind and earthquake for all loading amplitudes and frequencies. Xu et al. [16,17] utilized the viscoelastic damper to improve the seismic performance of the concrete frame structures. The design parameters and installation positions of the viscoelastic dampers are optimized, and shaking table tests of the structure models with and without dampers are carried out to validate the effectiveness of the dampers.

It can be seen that the mechanical properties and energy dissipation of the viscoelastic damper are greatly influenced by the excitation frequency, displacement amplitude and ambient temperature. It is important to select the appropriate mathematical model to describe the dynamic behavior of the viscoelastic damper in design and application procedures. Generally, the traditional viscoelastic mathematical models including the Kelvin model, Maxwell model, the generalized viscoelastic models, etc. are used to capture the properties of the viscoelastic materials [18–20]. Bagley et al. [21] and Meral et al. [22] employed the fractional calculus to model the constitutive relations of the viscoelastic materials. Gandhi et al. [23] used the standard linear solid model to simulate the nonlinear viscoelastic behaviors of the viscoelastic damper with dual-frequency excitations. Tsai et al. [7] proposed the finite element model which can consider the strain/displacement amplitude, frequency and ambient temperature influence on the mechanical properties of the viscoelastic dampers. Lewandowski et al. [24] utilized the generalized Kelvin and Maxwell model together with the W-L-F equation to characterize the properties of the viscoelastic damper considering the frequency and temperature influence. Xu et al. [25] theoretically and experimentally studied the temperature and displacement affection of viscoelastic dampers.

It also can be found that many scholars have paid attention to the influence of ambient temperature on the properties of viscoelastic dampers. However, the self-generated heating and temperature increment influence have received little attention [26–30]. Drozdov et al. [31] discussed the molecular chain fracture and deformation phenomenon of viscoelastic materials and studied the self-heating effects on dynamic properties of the viscoelastic material. Inaudi et al. [32] experimentally studied the mechanic properties change of the viscoelastic damper caused by heat generation during cyclic external loading, and the seismic responses of the structure with supplemental viscoelastic dampers considering self-generated heating are investigated by numerical simulation. Rodas et al. [33] formulated a thermo-visco-hyperelastic constitutive model to describe the self-heating process of viscoelastic materials with cyclic loadings. The finite-element-based simulations are conducted and compared with the experimental results.

In the present paper, dynamic properties tests of the sandwich viscoelastic damper at different environmental temperatures are carried out. The equivalent fractional Kelvin model is introduced to describe the dynamic properties and energy dissipation capability of the viscoelastic damper. The proposed model can characterize the mechanical behavior of the viscoelastic damper with varying frequencies and temperatures. The self-heating phenomenon of viscoelastic dampers is studied with numerical simulations. The dynamic properties and energy dissipation variations of the viscoelastic damper with different sizes and self-heating processes are analyzed. This demonstrates that the dynamic properties of the viscoelastic damper are significantly affected by temperature, excitation frequency and the internal self-generated heating.

2. Performance Tests

In order to better study the mechanical properties and energy dissipation of the sandwich viscoelastic damper with different temperatures, the dynamic properties tests of the sandwich viscoelastic damper at different temperatures (from 5 °C to 20 °C) are conducted. The results show that the viscoelastic damper has better performance of dynamic properties and energy dissipation capacities at low temperature. The dynamic parameters, including the storage modulus, loss factor, equivalent stiffness and equivalent damping, decrease with increasing ambient temperature.

2.1. Test Process

The sandwich viscoelastic damper consists of two viscoelastic material layers and three steel plates. The shear area of the viscoelastic damper is 60 mm × 50 mm, and the thickness of shear layer is 10 mm. The viscoelastic material is developed independently based on the nitrile rubber [11], and the steel type for the steel plates is Q235. The steel plates and viscoelastic layers of the damper are closely fixed with each other by chemical bonding in the vulcanization process and deform in different directions under cyclic external loading. The mechanical energy generated from external loading can be dissipated by the shear deformation of viscoelastic layers, and some parts of the mechanical energy are dissipated into the air in heat form. The schematic picture and photo of the viscoelastic damper are given in Figure 1a,b.

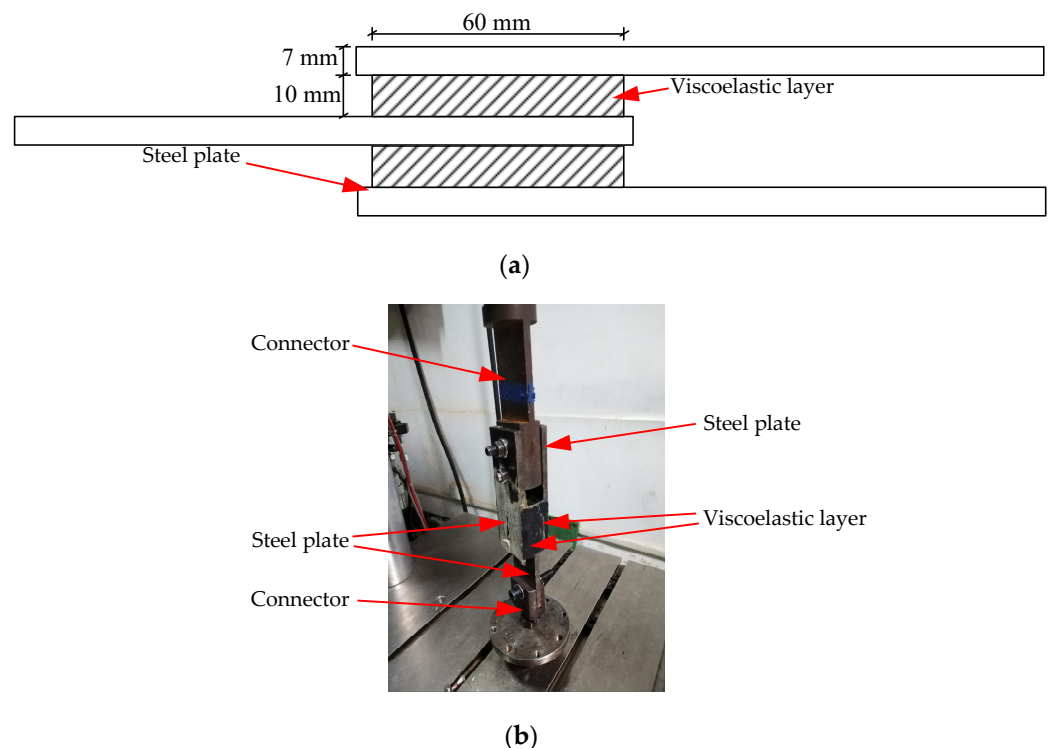


Figure 1. Photo of the viscoelastic damper.

To study the influence of ambient temperature on the dynamic properties and energy dissipation capability of the sandwich viscoelastic damper, the dynamic properties tests are conducted with a multipurpose universal servohydraulic LFV 100kN test series manufactured by *w + b* company, Switzerland, as seen in Figure 2a. Each test of the viscoelastic damper is carried out under 5 cycles of sinusoidal displacement loading $u_d = u_0 \sin(2\pi ft)$, where u_0 represents the amplitude of the displacement loading, and f denotes the loading frequency. The displacement and frequency in each test can be recorded directly in the control and data acquisition system with the DION 7 software. All the test conditions are given in Table 1. A temperature controlling device, as shown in Figure 2a,b, is used to adjust the environmental temperature of the damper.

Table 1. Test conditions of the sandwich viscoelastic damper.

Temperature T (°C)	Displacement Amplitude d (mm)	Frequency f (Hz)	Cyclic Number
−5, 0, 10, 15, 20	1.0, 2.0	0.1, 0.2, 0.5, 1.0	5

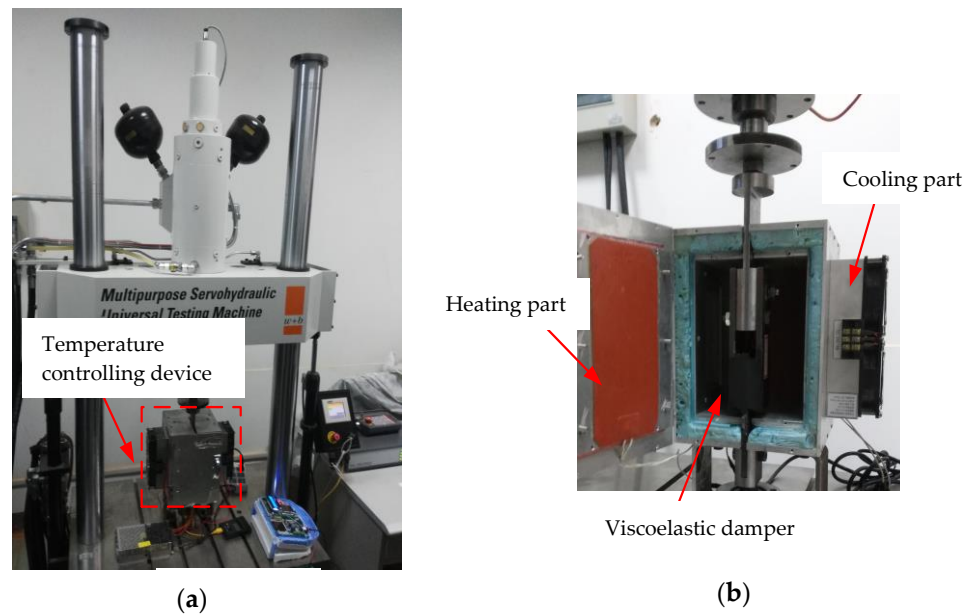


Figure 2. Properties test of the viscoelastic damper: (a) tests of the viscoelastic damper; (b) temperature controlling device.

2.2. Test Results

In order to obtain the dynamic performance and energy dissipation indices of the sandwich viscoelastic damper, the fourth loop of the force–displacement curves at each test condition is selected and analyzed. The representative hysteresis curves of the sandwich viscoelastic damper are shown in Figure 3.

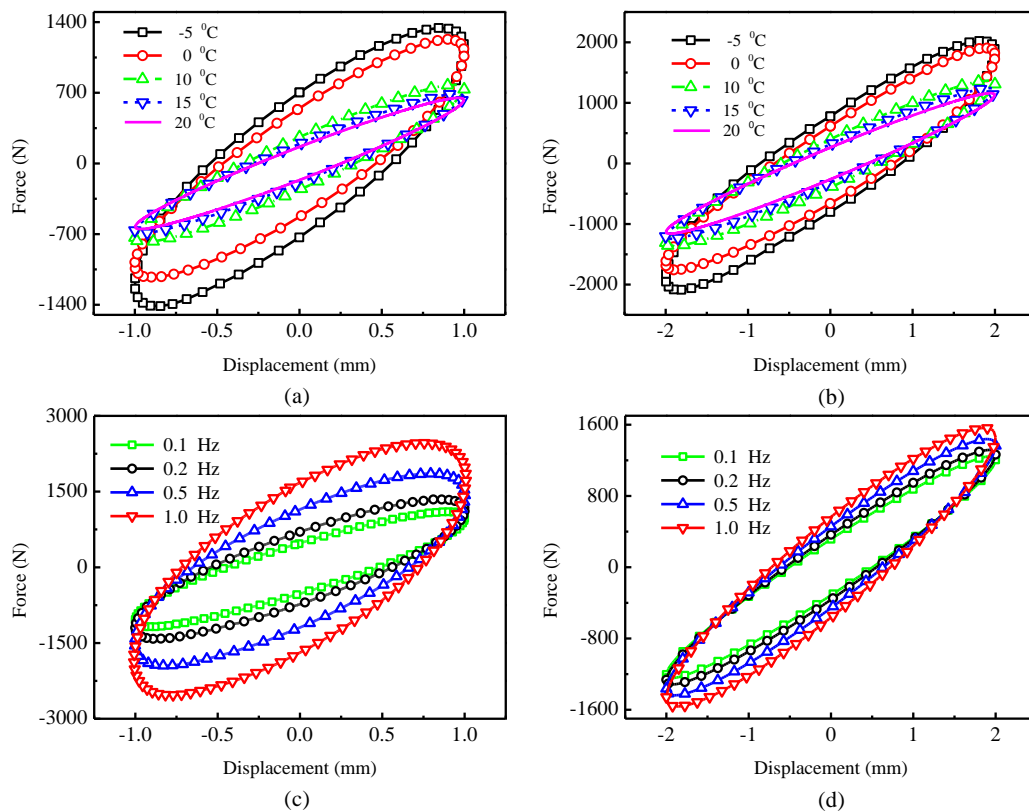


Figure 3. Representative force-displacement curves of the viscoelastic damper: (a) $d = 1.0$ mm, $f = 0.2$ Hz; (b) $d = 2.0$ mm, $f = 0.1$ Hz; (c) $T = -5$ °C, $d = 1.0$ mm; (d) $T = 15$ °C, $d = 2.0$ mm.

Figure 3a,b presents the variations of the force–displacement hysteresis curves of the damper with changing ambient temperature (from $-5\text{ }^{\circ}\text{C}$ to $20\text{ }^{\circ}\text{C}$) at the test conditions of displacement 1 mm and frequency 0.2 Hz and displacement 2 mm and frequency 0.1 Hz , respectively. The sandwich viscoelastic damper has fuller hysteresis curves and larger elliptical slopes at low temperatures. As the temperature increases from $-5\text{ }^{\circ}\text{C}$ to $20\text{ }^{\circ}\text{C}$, the fullness and slope of the hysteresis curves gradually decrease.

Figure 3c,d gives the variations of the force–displacement curves of the damper with different loading frequencies (from 0.1 Hz to 1.0 Hz) with the test conditions of temperature $-5\text{ }^{\circ}\text{C}$ and displacement 1.0 mm , and temperature $15\text{ }^{\circ}\text{C}$ and displacement 2.0 mm , respectively. The fullness and slope of the hysteresis curves gradually increase with increasing frequencies. As the fullness and slope of the hysteretic curves are greatly related to the stiffness and energy dissipation capacity of the viscoelastic damper, it can be concluded that the stiffness and energy dissipation capacity of the sandwich viscoelastic damper decrease with increasing temperature and increase with increasing frequency. The sandwich viscoelastic damper has better dynamic properties and energy dissipation ability at low temperature than that at high temperature.

Under the sinusoidal displacement loading $u_d = u_0 \sin(2\pi ft)$, the force–displacement hysteretic curve of the viscoelastic damper at each test condition can be treated as a full ellipse [8], as seen in Figure 4.

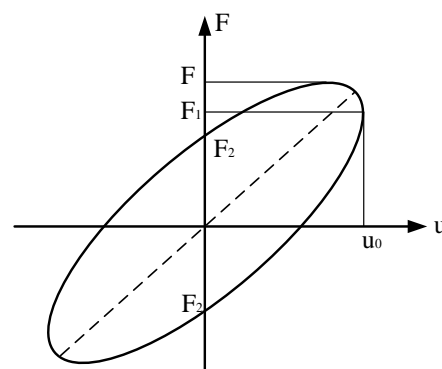


Figure 4. Hysteretic curve simplification of the viscoelastic damper.

The full ellipse can be expressed as

$$\left(\frac{F_d - K_e u_d}{\eta K_e u_0}\right)^2 + \left(\frac{u_d}{u_0}\right)^2 = 1 \quad (1)$$

In Equation (1), F_d and u_d denotes the damping force and corresponded displacement of the damper, respectively; $K_e = \frac{F_1}{u_0}$, which represents the equivalent stiffness, u_0 , and F_1 denotes the maximum displacement and the damping force at u_0 ; F_2 is the damping force of the damper when the displacement is zero, and F represents the biggest damping force of the viscoelastic damper on one hysteretic curve. Based on the hysteretic curve simplification of the viscoelastic damper, the dynamic properties and energy dissipation indices, such as the storage modulus G_1 , the loss factor η , the equivalent stiffness K_e and equivalent damping C_e of the viscoelastic damper can be expressed as [34]

$$G_1 = \frac{F_1 h_v}{n_v A_v u_0} \quad (2)$$

$$\eta = \frac{F_2}{F_1} \quad (3)$$

$$K_e = \frac{n_v G_1 A_v}{h_v} \quad (4)$$

$$C_e = \frac{\eta n_v G_1 A_v}{\omega h_v} \quad (5)$$

where n_v denotes the number of viscoelastic layers, A_v and h_v represent the shear area and thickness of each viscoelastic layer, and $\omega = 2\pi f$.

For the sandwich type viscoelastic damper utilized in this test, $n_v = 2$, $A_v = 50 \times 60 = 3000 \text{ mm}^2$ and $h_v = 10 \text{ mm}$. Then, together with Equations (2)–(5), the storage modulus G_1 , the loss factor η , the equivalent stiffness K_e and equivalent damping C_e at each test condition can be calculated. To briefly show the dynamic properties and energy dissipation performance of the viscoelastic damper, only the dynamic parameters with displacement 1.0 mm are given and clearly pictured in Figure 5. The details of the dynamic parameters are shown in Table 2.

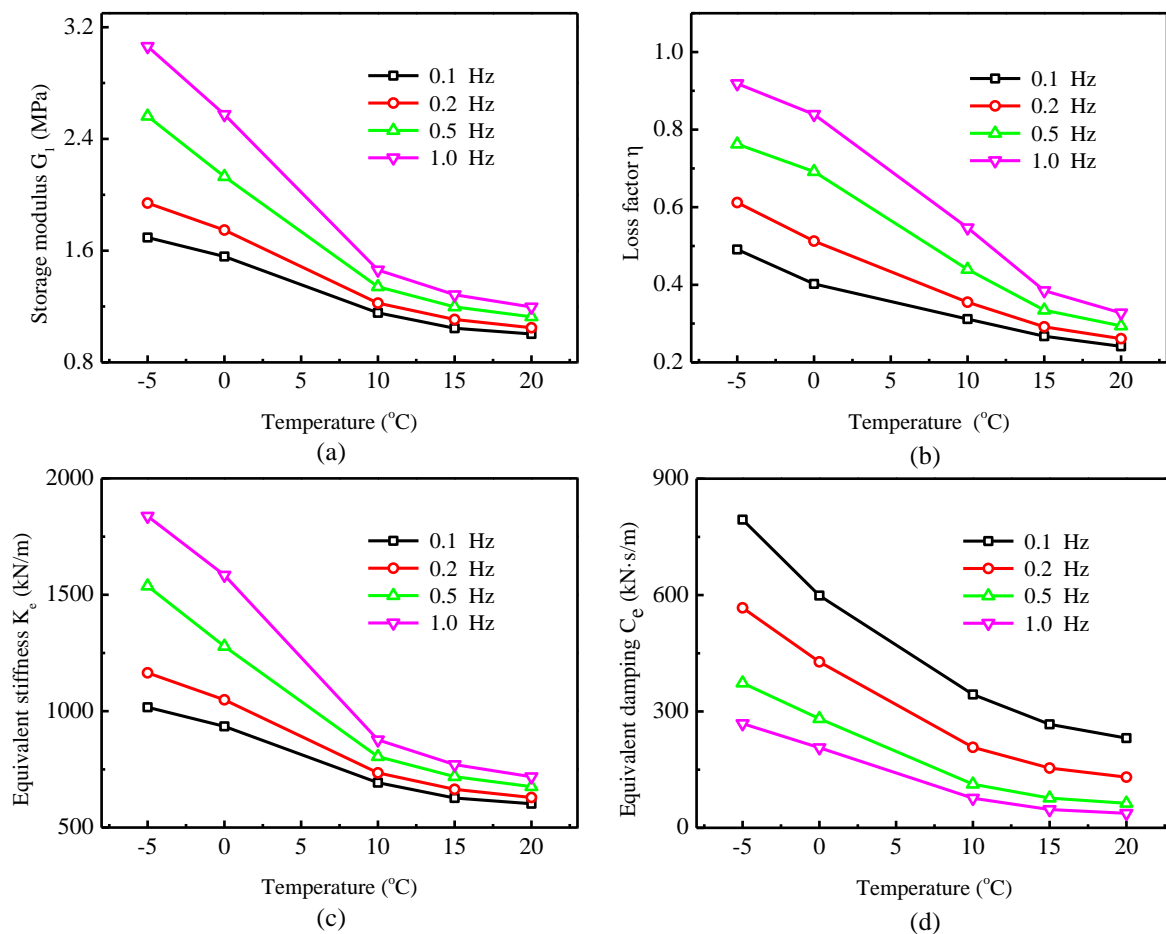


Figure 5. Parameters of the viscoelastic damper with displacement 1.0 mm: (a) storage modulus; (b) loss factor; (c) equivalent stiffness; (d) equivalent damping.

Figure 5 presents the characteristic parameters of the sandwich viscoelastic damper with changing temperature from $-5 \text{ }^\circ\text{C}$ to $20 \text{ }^\circ\text{C}$ when the displacement amplitude is 1.0 mm. It is easy to see that the storage modulus, loss factor, equivalent stiffness and equivalent damping decrease significantly by increasing the temperature, especially at low temperatures (from $-5 \text{ }^\circ\text{C}$ to $10 \text{ }^\circ\text{C}$). Taking 1.0 Hz as an example, the storage modulus decreases by 15.91% in the range of $-5 \text{ }^\circ\text{C}$ to $0 \text{ }^\circ\text{C}$, decreases by 43.25% in the range of $0 \text{ }^\circ\text{C}$ to $10 \text{ }^\circ\text{C}$, decreases by 12.14% in the range of $10 \text{ }^\circ\text{C}$ to $15 \text{ }^\circ\text{C}$ and decreases by 6.8% in the range of $15 \text{ }^\circ\text{C}$ to $20 \text{ }^\circ\text{C}$. The loss factor decreases by 8.63% in the range of $-5 \text{ }^\circ\text{C}$ to $0 \text{ }^\circ\text{C}$, decreases by 34.86% in the range of $0 \text{ }^\circ\text{C}$ to $10 \text{ }^\circ\text{C}$, decreases by 29.62% in the range of $10 \text{ }^\circ\text{C}$ to $15 \text{ }^\circ\text{C}$, and decreases by 14.91% in the range of $15 \text{ }^\circ\text{C}$ to $20 \text{ }^\circ\text{C}$. The equivalent stiffness decreases by 13.77% in the range of $-5 \text{ }^\circ\text{C}$ to $0 \text{ }^\circ\text{C}$, decreases by 44.66% in the range of

0 °C to 10 °C, decreases by 12.14% in the range of 10 °C to 15 °C, and decreases by 6.8% in the range of 15 °C to 20 °C. The equivalent damping decreases by 23.17% in the range of −5 °C to 0 °C, decreases by 63.03% in the range of 0 °C to 10 °C, decreases by 38.17% in the range of 10 °C to 15 °C, and decreases by 20.7% in the range of 15 °C to 20 °C.

Table 2. Dynamic parameters of the viscoelastic damper with displacement 1.0 mm.

Temperature T (°C)	Frequency f (Hz)	Storage Modulus G_1 (MPa)	Loss Factor η	Equivalent Stiffness K_e (KN/m)	Equivalent Damping C_e (KN·s/m)
−5	0.1	1.69	0.49	1016.57	794.49
	0.2	1.94	0.61	1164.49	566.99
	0.5	2.56	0.76	1537.5	373.22
	1.0	3.06	0.92	1837.54	268.65
0	0.1	1.56	0.4	934.58	598.56
	0.2	1.75	0.51	1048.61	427.84
	0.5	2.13	0.69	1278.11	281.38
	1.0	2.64	0.82	1584.48	206.41
10	0.1	1.15	0.31	692.89	343.78
	0.2	1.22	0.36	734.79	207.68
	0.5	1.34	0.44	804.67	112.59
	1.0	1.46	0.55	876.86	76.31
15	0.1	1.04	0.27	626.66	266.7
	0.2	1.11	0.29	664.27	154.16
	0.5	1.2	0.33	718.45	76.54
	1.0	1.28	0.38	770.4	47.19
20	0.1	1.0	0.24	602.2	231.29
	0.2	1.05	0.26	628.87	130.71
	0.5	1.13	0.29	675.75	63.24
	1.0	1.2	0.33	718.02	37.42

This phenomenon indicates that the dynamic performance of the sandwich viscoelastic damper greatly decreases with increasing temperature, and the damper has better energy dissipation capacity at lower temperature. It can also be found that the storage modulus, loss factor, and equivalent stiffness increase when the excitation frequency increases, and equivalent damping decreases with the increasing frequency.

3. Mathematical Modeling

As seen in dynamic properties tests, the mechanical properties and energy dissipation capability of the sandwich viscoelastic damper are significantly affected by the ambient temperature and loading frequency. The equivalent fractional Kelvin model is employed in this section to describe the mechanical and damping properties variation of the sandwich viscoelastic damper with different ambient temperatures and loading frequencies. The fractional Kelvin model consists of one spring element and a fractional dashpot in parallel [25], as seen in Figure 6.

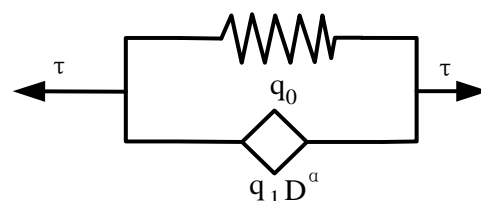


Figure 6. Fractional Kelvin model.

The constitutive relation of the fractional Kelvin model can be written as

$$q_0\gamma + q_1D^\alpha\gamma = \tau \quad (6)$$

where q_0 denotes the modulus of the spring element, and q_1 denotes the damping of fractional dashpot; γ is the shear strain, and τ is the shear stress; α is the fractional order derivative, and $0 < \alpha < 1.0$. Applying the Fourier transform to Equation (6), we can obtain that

$$G^* = q_0 + q_1(j\omega)^\alpha \quad (7)$$

where G^* is the shear modulus of fractional Kelvin model in complex form, and j represents the unit complex number. By decomposing the complex modulus into two parts, the real part and the imaginary part, the storage modulus, shear modulus and loss factor of the viscoelastic material can be obtained as

$$G_1 = \text{Re}(G^*) = q_0 + q_1\omega^\alpha \cos(\alpha\pi/2) \quad (8)$$

$$G_2 = \text{Im}(G^*) = q_1\omega^\alpha \sin(\alpha\pi/2) \quad (9)$$

$$\eta = q_1\omega^\alpha \sin(\alpha\pi/2) / [q_0 + q_1\omega^\alpha \cos(\alpha\pi/2)] \quad (10)$$

In the above equations, G_1 , G_2 and η represent the storage modulus, loss modulus and loss factor of viscoelastic materials, respectively.

When the ambient temperature is around T_g to $T_g + 100$ °C, the temperature and frequency influences on the dynamic properties of the viscoelastic damper have an equivalent relationship, and the dynamic properties of viscoelastic damper at high temperature are equivalent to those at low frequency, which can be described by the temperature–frequency equivalent theory [11,20,25], as shown in Equation (11)

$$G_1(\omega, T) = G_1(\alpha_T\omega, T_0); \eta(\omega, T) = \eta(\alpha_T\omega, T_0) \quad (11)$$

where T_g is the glass transition temperature, T_0 is the reference temperature, and α_T can be written as

$$\alpha_T = 10^{-12(T-T_0)/[525+(T-T_0)]} \quad (12)$$

From Equation (12), it can be seen that the temperature–frequency equivalent theory is an application of the W-L-F equation [24,35] in viscoelastic damping device studies. By considering the temperature–frequency equivalent theory together with Equations (8)–(10), the equivalent fractional Kelvin model can be obtained as

$$G_1 = q_0 + q_1(\alpha_T\omega)^\alpha \cos(\alpha\pi/2) \quad (13)$$

$$G_2 = q_1(\alpha_T\omega)^\alpha \sin(\alpha\pi/2) \quad (14)$$

$$\eta = q_1(\alpha_T\omega)^\alpha \sin(\alpha\pi/2) / [q_0 + q_1(\alpha_T\omega)^\alpha \cos(\alpha\pi/2)] \quad (15)$$

Equations (13) to (15) are expressions of the equivalent fractional Kelvin model. It can effectively characterize the affection of ambient temperatures and loading frequencies on dynamic properties and energy dissipation ability of viscoelastic materials and dampers.

To further reveal the temperature influence on dynamic properties and energy dissipation of the damper with equivalent fractional Kelvin model, the experimental results of the dynamic properties tests are used to determine the model parameters. As Equations (12)–(15) could not reflect the displacement amplitude influence and the fact that only the tests with displacement 1.0 mm and 2.0 mm are conducted, the test results with displacement 1.0 mm and 2.0 mm are treated separately. Only parts of the test data are selected for parameters determination. When the displacement is 1.0 mm, the parameters of the equivalent fractional Kelvin model can be obtained as, $q_0 = 6.69 \times 10^5$, $q_1 = 98.97$, $\alpha = 0.4781$, and $T_0 = 490.52$ K. When the displacement is 2.0 mm, $q_0 = 6.2 \times 10^5$, $q_1 = 420.52$, $\alpha = 0.4355$, and $T_0 = 479.02$ K. The experimental and numerical results comparisons of the equivalent fractional Kelvin model of the sandwich viscoelastic damper with displacement 1.0 mm and 2.0 mm are plotted in Figure 7.

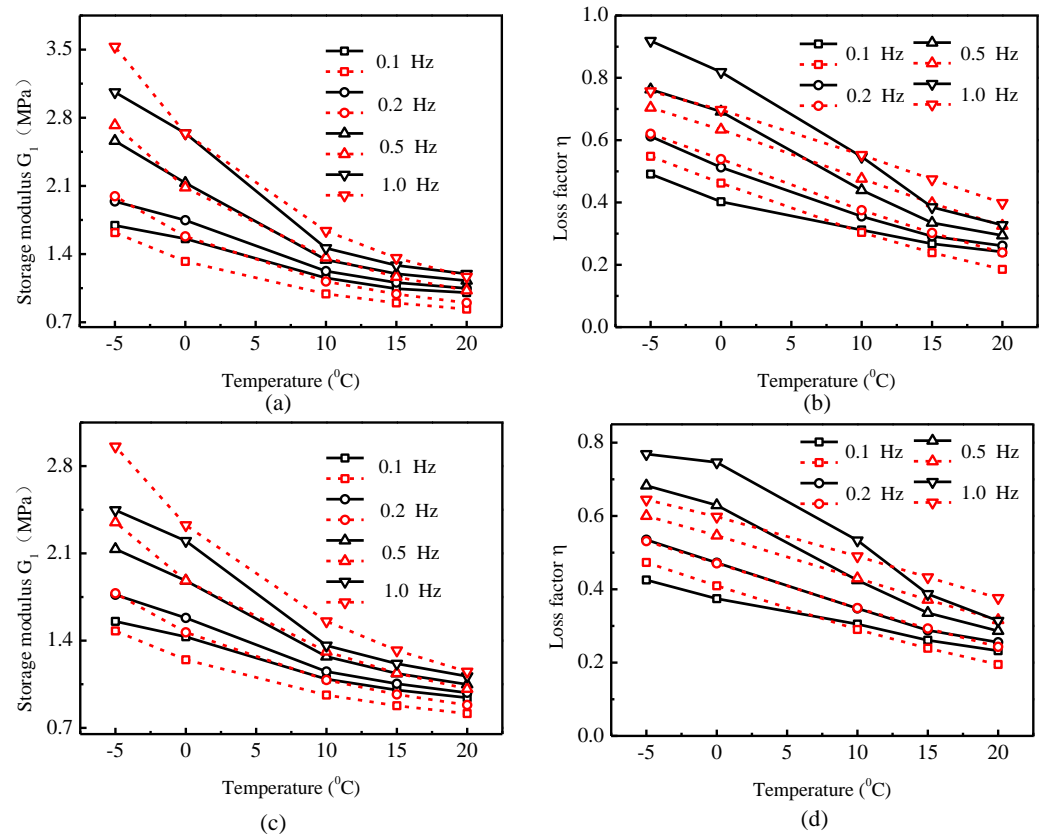


Figure 7. Experimental and numerical results comparisons of equivalent fractional Kelvin model for the sandwich viscoelastic damper: (a) storage modulus, $d = 1.0$ mm; (b) loss factor, $d = 1.0$ mm; (c) storage modulus, $d = 2.0$ mm; (d) loss factor, $d = 2.0$ mm.

The equivalent fractional Kelvin model can well characterize the mechanical properties and energy dissipation capacity of the sandwich viscoelastic damper with varying environmental temperatures. Taking a displacement of 2.0 mm as an example, the experimental and numerical data are given in Table 3. The numerical results agree well with the experimental results at different temperatures, and the errors do not exceed 21%. For storage modulus, the maximum error is 20.87% with an ambient temperature of -5 °C and a frequency 1.0 Hz; the experimental and numerical results are 2.45 MPa and 2.96 MPa, respectively. For loss factor, the maximum error is 19.75% with an ambient temperature of 20 °C and a frequency of 1.0 Hz; the experimental and numerical results are 0.314 and 0.376, respectively.

Table 3. Comparison of experimental and numerical results of the equivalent fractional Kelvin model when $d = 2.0$ mm.

Temperature T (°C)	Frequency f (Hz)	Experimental Results		Numerical Results	
		Storage Modulus G_1 (MPa)	Loss Factor η	Storage Modulus G_1 (MPa)	Loss Factor η
−5	0.1	1.55	0.43	1.48	0.47
	0.2	1.77	0.54	1.78	0.53
	0.5	2.13	0.68	2.35	0.60
	1.0	2.45	0.77	2.96	0.64
0	0.1	1.43	0.37	1.25	0.41
	0.2	1.58	0.47	1.47	0.47
	0.5	1.88	0.63	1.88	0.54
	1.0	2.2	0.75	2.33	0.60

Table 3. Cont.

Temperature T (°C)	Frequency f (Hz)	Experimental Results		Numerical Results	
		Storage Modulus G_1 (MPa)	Loss Factor η	Storage Modulus G_1 (MPa)	Loss Factor η
10	0.1	1.09	0.30	0.96	0.29
	0.2	1.15	0.35	1.08	0.35
	0.5	1.27	0.42	1.31	0.43
	1.0	1.36	0.53	1.56	0.49
15	0.1	1.0	0.26	0.88	0.24
	0.2	1.05	0.29	0.97	0.29
	0.5	1.14	0.34	1.14	0.37
	1.0	1.22	0.39	1.32	0.43
20	0.1	0.94	0.23	0.82	0.19
	0.2	0.98	0.26	0.88	0.24
	0.5	1.05	0.29	1.01	0.32
	1.0	1.11	0.31	1.15	0.38

4. Self-Generated Heating of the Sandwich Viscoelastic Damper

The dynamic properties and energy dissipation capability of viscoelastic materials are significantly affected by ambient temperature. In the design and seismic analysis of building structures installed with viscoelastic dampers, the influence of ambient temperature is always ignored. During the service life of the viscoelastic damper, the ambient temperature is not stable. At the same time, the external mechanical energy could be converted into heat through the shear deformation of the viscoelastic layers, which causes the internal temperature to rise and affects the dynamic performance of the damper. In this section, the self-heating phenomenon of the sandwich viscoelastic damper is investigated. The initial temperature of the whole damper and ambient temperature is taken as 10 °C.

Considering that the heat generation rate of the viscoelastic material is affected by ambient temperature and ignoring the thermoelastic coupling effect (thermal expansion), the heat transfer equation of the viscoelastic layer in the damper can be written as [31]

$$q_g + k\nabla^2 T(t, x, y, z) = \rho c_p \dot{T}(t, x, y, z) \quad (16)$$

with the boundary conditions

$$\begin{cases} T = T_0 & \text{in } \partial\Omega_D \\ q = q_0 & \text{in } \partial\Omega_N \\ q = h(T - T_\infty) & \text{in } \partial\Omega_C \end{cases} \quad (17)$$

where, k , ρ , and c_p represent the thermal conductivity, density and specific heat capacity of the materials, respectively. The value of $k\nabla^2 T(t, x, y, z)$ can be obtained by applying Fourier's law to a certain volume; $\rho c_p \dot{T}(t, x, y, z)$ represents the heat restored inside the material. T_0 denotes the temperature loading on the boundary of the domain Ω_D , q_0 denotes the heat flow on the boundary domain Ω_N , h represents the heat convection coefficient between the boundary domain Ω_C and the surroundings, T_∞ is the ambient temperature, q_g is the heat generation rate of the viscoelastic material and has the form

$$q_g = \beta_t \dot{w}_m \quad (18)$$

where β_t is the thermal conversion ratio, which means the fraction of heat energy converted from the dissipated mechanical energy through shear deformation of the viscoelastic materials, \dot{w}_m is the dissipated external mechanical power, and $(1 - \beta_t)\dot{w}_m$ represents

the storage rate of the energy stored inside the viscoelastic material by micro-structural changes. \dot{w}_m has the form [31]

$$\dot{w}_m(t, \omega, T) = -\omega G_2(\omega, T) \bar{C} \varepsilon_0^T(t, \omega, T) \sin^2(\omega t + \delta) \quad (19)$$

where $C(t, \omega, T) = G(t, \omega, T) \bar{C}$, $G(t, \omega, T) = G_1(t, \omega, T) + G_2(t, \omega, T)j$; ε_0 denotes the strain of the viscoelastic materials, and δ presents the phase angle of the stress and strain.

Based on the abovementioned heat generate and transfer theories, the finite-element simulation with a two-dimensional (2-D) model is conducted to study the self-heating phenomenon. The 2-D model of the viscoelastic damper is shown in Figure 8.

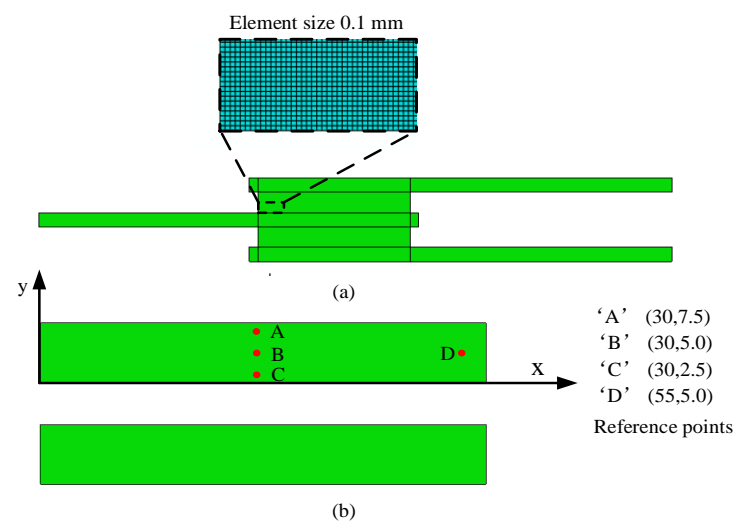


Figure 8. 2-D model of the sandwich viscoelastic damper: (a) 2-D model and local mesh structure of the viscoelastic damper; (b) the local coordinate in viscoelastic layers and the reference points.

In the finite element simulation, the displacement amplitude of the viscoelastic damper is 1.0 mm, and the ‘Coupled-Temperature-Displacement’ time step is employed to simulate the thermo-viscoelastic behaviors of the material. The ‘CPE4T’ planar element type is used for meshing of viscoelastic damper. In order to avoid the element distortion with a large number of loading cycles, the element size of the viscoelastic layer is selected as 0.1 mm, while the element size of the steel plate is getting larger and larger when it is gradually getting away from the viscoelastic materials. The total number of finite elements of the 2-D model is 255428. In order to better understand the temperature rising at different positions of the viscoelastic layer, four reference points ‘A’, ‘B’, ‘C’ and ‘D’ are selected in the viscoelastic layer, as seen in Figure 8b. A local coordinate system is defined in the upper viscoelastic layer, and the coordinates of the reference points ‘A’, ‘B’, ‘C’ and ‘D’ are (30,7.5), (30,5.0), (30,2.5) and (55,5.0), respectively.

In this section, the temperature influence on the material properties should be considered to simulate the thermo-viscoelastic behavior of the viscoelastic damper. In ABAQUS, the Prony series by default defines the viscoelastic properties of the viscoelastic material. The W-L-F equation $\log \alpha_T = -C_1(T - T_0)(C_2 + T - T_0)$ [24,35] can be utilized to describe the temperature influence. C_1 and C_2 are material constants. With the Prony series and W-L-F equation, the viscoelastic properties of the viscoelastic material can be obtained and shown in Table 4 [35]. The Poisson’s ratio of the viscoelastic material is 0.49, and the modulus and Poisson’s ratio of the steel plate is 210 GPa and 0.3. The thermal properties of the viscoelastic layer and steel plate are shown in Table 5 [36,37].

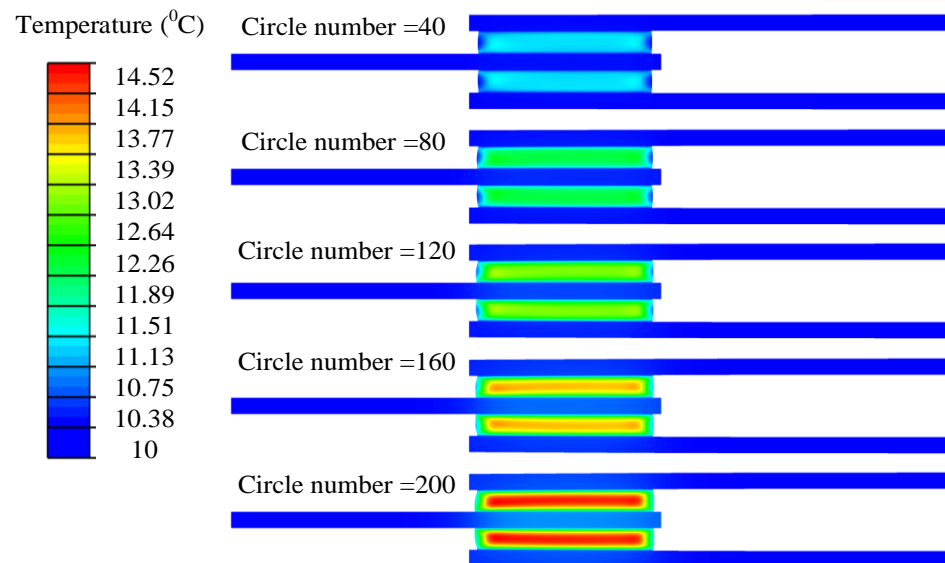
Table 4. Viscoelastic parameters determined with Prony series and W-L-F equation in ABAQUS ($n = 4$), when $d = 1.0$ mm.

G_0 (MPa)	T_0 (K)	g_1	g_2	g_3	g_4
13.104	486.9721	0.3485	0.0357	0.0546	0.502
τ_1	τ_2	τ_3	τ_4	C_1	C_2
1.9055×10^{-11}	7.0947×10^{-8}	4.3061×10^{-9}	2.5573×10^{-10}	12	525

Table 5. Thermal properties parameters of the viscoelastic layers and steel plates.

Material	Thermal Conductivity κ ($w \cdot m/K$)	Density ρ (kg/m^3)	Specific Heat Capacity C_E ($J/(kg \cdot K)$)	Thermal Expansion Coefficient α_t (K^{-1})
Viscoelastic material	0.16	990	2000	1.15×10^{-4}
Steel plate	19.5	7970	561	1.77×10^{-5}

The heat convection coefficient h between the surfaces of the viscoelastic damper and surrounding environment is taken as 6 ($w \cdot m^2/K$) [38]. The model of the viscoelastic damper is subjected to 200 cycles of displacement loading $u_d = u_0 \sin(2\pi ft)$. When the displacement amplitude is 1.0 mm and the loading frequency is 5.0 Hz, the temperature contours of the viscoelastic damper at different loading circles are shown in Figure 9.

**Figure 9.** The temperature contour of the viscoelastic damper at different loading circles ($d = 1.0$ mm, and $f = 5.0$ Hz).

The temperature of the viscoelastic materials increases gradually as the number of loading circles increases. The temperature of the upper and lower layers of the viscoelastic material is symmetrically distributed with respect to the intermediate steel plate. A higher temperature area is formed within a certain region inside the viscoelastic layers. After 200 cycles of sinusoidal displacement loading, the local temperature at the center of the viscoelastic layer reaches to 14.52 °C, and the maximum increment is 4.52 °C.

Figure 10 shows the temperature increment at the reference points with increasing loading circle numbers. The temperature rising processes at reference points 'A', 'B', 'C' and 'D' are different, which is caused by the difference in heat generation and transfer due to the change of position and boundary conditions. With the same loading circle, the

temperature increment increases when the loading frequency goes up. The temperature with larger frequency is obviously higher than that with lower frequency. The reason is that the mechanical properties such as the modulus of the viscoelastic material increases with increasing frequency. The mechanical energy dissipation and heat generation rates in each single loading cycle of the viscoelastic material increase with increasing frequency. Take reference point 'B' as an example, at the 140th loading circle, the temperature is 11.06, 13.27, 14.88 and 16.08 °C with frequency 1.0, 5.0, 10.0 and 20.0 Hz. The temperature increment compared to initial temperature is 1.06, 3.27, 4.88 and 6.08 °C, respectively.

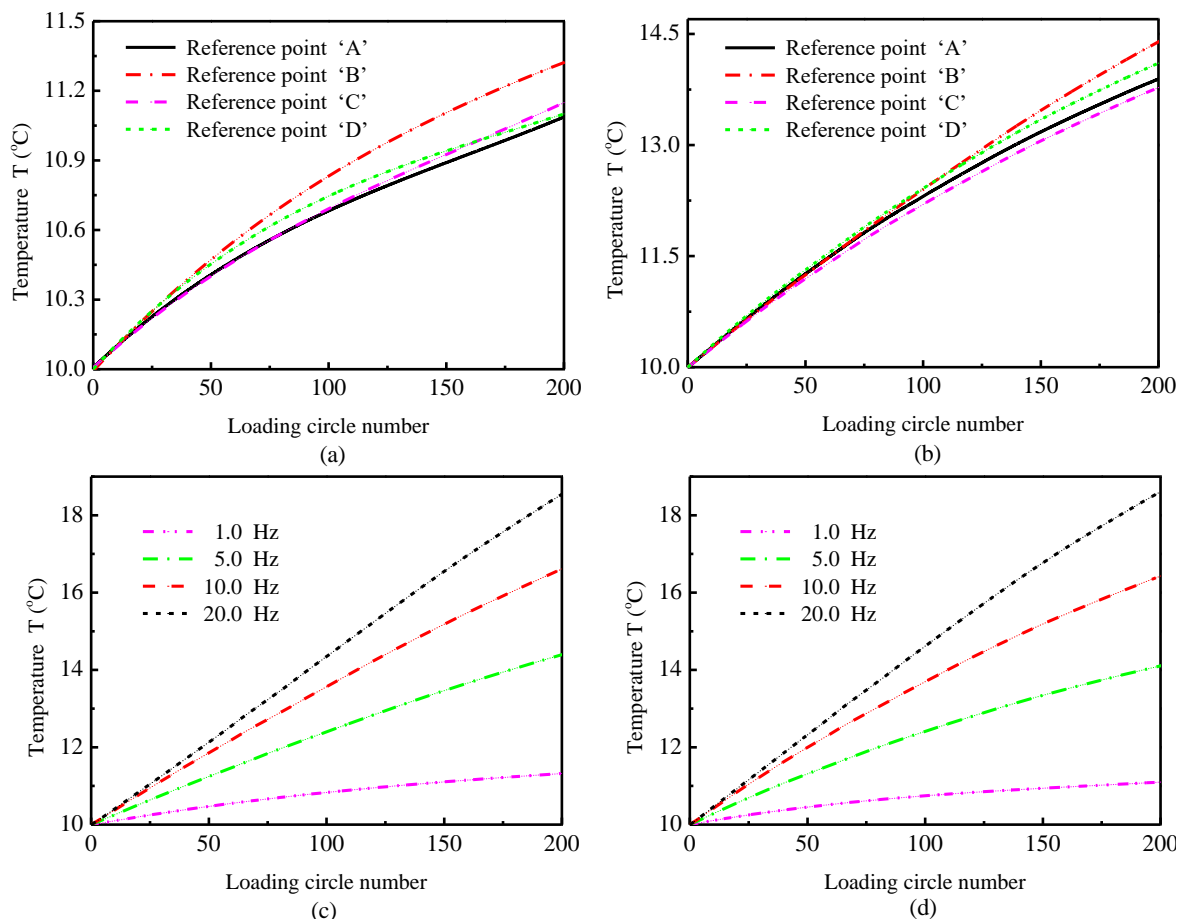


Figure 10. The temperature increment at the reference points with increasing loading circle numbers: (a) $f = 1.0$ Hz; (b) $f = 5.0$ Hz; (c) Reference point 'B'; (d) Reference point 'D'.

As the mechanical properties and energy dissipation capacity of the viscoelastic damper are greatly affected by ambient temperature, it is necessary to study the self-heating influence on the dynamic behaviors of the viscoelastic damper. Figure 11 gives the force-displacement hysteretic curve, damping force, storage modulus and loss factor variations of the sandwich viscoelastic damper at frequencies 1.0, 5.0, 10.0 and 20.0 Hz with loading circle numbers within 100. Figure 11a,b reveals that the fullness and slope of the force-displacement hysteretic curves change apparently when the loading circles increase. The damping force with circles from 95 to 100 is much less than that with circles from 1 to 5, which can be attributed to the modulus and stiffness decrease caused by the self-heating inside the viscoelastic layer. Taking the 5th and 95th loading circles at 5.0 Hz as an example, the peak force at unit width of the viscoelastic damper is 38.8438 N and 34.7891 N, respectively. The peak force at the 95th circle is 10.44% lower than that at the 5th circle.

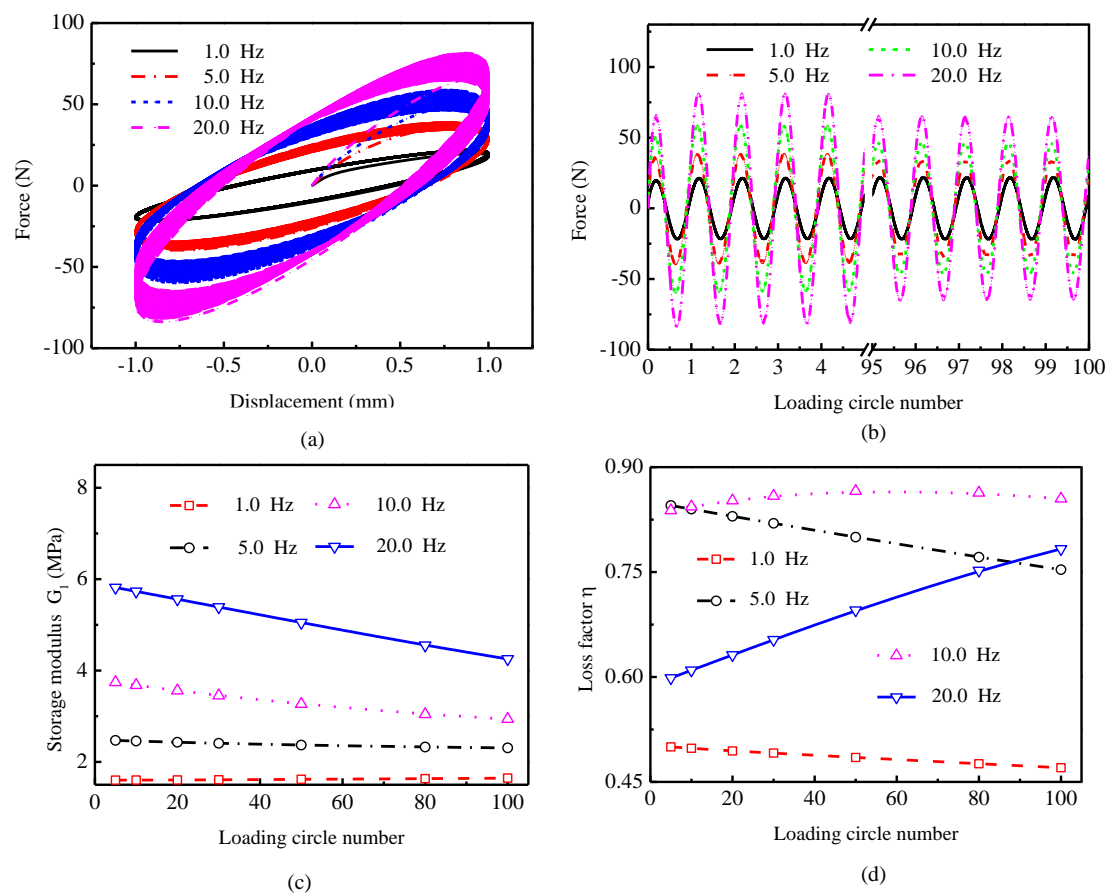


Figure 11. Mechanical properties variation of the sandwich viscoelastic damper with increasing loading circle numbers: (a) force-displacement hysteresis curve; (b) damping force; (c) storage modulus; (d) loss factor.

The FEA results of the storage modulus and loss factor of the viscoelastic damper are shown in Figure 11c,d, and the storage modulus decreases when the loading cycles increase. The loss factor decreases as the number of loading circle increases at low frequencies (1.0 Hz and 5.0 Hz); and increases with the increasing loading cycles at high frequencies (10.0 Hz and 20.0 Hz). Taking the 10th, 30th, 50th and 80th circles with 10 Hz as examples, the FEA results of storage modulus are 3.6793, 3.4528, 3.2663 and 3.0417 MPa, respectively. It decreases by 6.16% in the range of the 10th to the 30th loading circles, decreases by 5.4% in the range of the 30th to the 50th loading circles and decreases by 6.88% in the range of the 50th to the 80th loading circles.

5. Conclusions

In the present work, dynamic properties tests of the sandwich viscoelastic damper at different ambient temperatures were conducted. The equivalent fractional Kelvin model was introduced to describe the thermo-viscoelastic behaviors of the viscoelastic damper. The self-heating phenomenon of the viscoelastic damper was investigated, and the finite element simulation was utilized to verify the self-heating influence on dynamic properties and energy dissipation capacity of the sandwich type viscoelastic damper.

Based on these studies some notable conclusions can be obtained as follows: ① The sandwich viscoelastic damper has perfect energy dissipation capacity, and the performance of the viscoelastic damper at low temperature is better than that at high temperature. Almost all the hysteresis curves of the sandwich viscoelastic damper are full ellipses, and the key energy dissipation parameter, loss factor η , reaches its maximum value near 1.0 with a temperature of -5°C and a frequency of 1.0 Hz. ② The storage modulus, loss factor, equivalent stiffness and equivalent damping decrease when the temperature increases,

and the storage modulus, loss factor, and equivalent stiffness increase with an increase in frequency, while the equivalent damping decreases with an increase in frequency. ③ The temperature inside the viscoelastic layers could be obviously increased during the cyclic displacement loading due to the self-generated heating. The parameters decrease importantly because of the internal temperature increment. When the displacement amplitude is 1.0 mm and the loading frequency is 5.0 Hz, the maximum temperature increment is 4.52 °C after 200 cyclic loadings with initial temperature 10 °C. When displacement is 1mm, and frequency is 10 Hz, the storage modulus changes from 3.6793 to 3.0417 MPa at the 10th and the 80th loading circles, decreasing by 17.33%.

In this paper, dynamic properties tests of the sandwich viscoelastic damper with different temperatures were carried out. The equivalent fractional order kelvin model was formulated to capture the temperature influence on dynamic properties. The Finite Element Analysis method is used to investigate the self-heating phenomena. The results reveal that the dynamic properties of the damper are significantly affected by temperature, excitation frequency and the internal self-generated heating.

Author Contributions: Conceptualization, Z.-D.X.; data curation, Y.X. and Y.-Q.G.; formal analysis, Y.X.; funding, acquisition, Z.-D.X.; investigation, Y.X. and X.H.; methodology, Z.-D.X.; resources, Z.-D.X.; software, Y.-R.D. and Q.-Q.L.; supervision, Y.-Q.G.; validation, Y.X., X.H., Y.-R.D. and Q.-Q.L.; writing—original draft, Y.X.; writing—review and editing, Z.-D.X. and Y.-Q.G. All authors have read and agreed to the published version of the manuscript.

Funding: This research was financially supported by the National Key R&D Programs of China with Grant Nos. 2016YFE0200500 and 2016YFE0119700, the Jiangsu Province International Cooperation Project with Grant No. BZ 2018058, the National Science Fund for Distinguished Young Scholars with Grant No. 51625803, the Program of Chang Jiang Scholars of Ministry of Education, National Natural Science Foundation of China with Grant No. 11572088.

Institutional Review Board Statement: Not applicable.

Informed Consent Statement: Not applicable.

Data Availability Statement: The data presented in this study are available on request from the corresponding author. The data are not publicly available due to the confidentiality requirements of the lab.

Acknowledgments: The authors are thankful for the help of Professor Yonggang Huang's research group in Northwestern University (Evanston, IL, 60201, U.S.)

Conflicts of Interest: The authors declare no conflict of interest. The funders had no role in the design of the study; in the collection, analyses or interpretation of data; in the writing of the manuscript or in the decision to publish the results.

References

1. Xu, Z.D.; Huang, X.H.; Xu, F.H.; Yuan, J. Parameters optimization of vibration isolation and mitigation system for precision platforms using non-dominated sorting genetic algorithm. *Mech. Syst. Signal Process.* **2019**, *128*, 191–201. [[CrossRef](#)]
2. Lu, Z.; Wang, Z.X.; Zhou, Y.; Lu, X.L. Nonlinear dissipative devices in structural vibration control: A review. *J. Sound Vib.* **2018**, *423*, 18–49. [[CrossRef](#)]
3. Rao, M.D. Recent applications of viscoelastic damping for noise control in automobiles and commercial airplanes. *J. Sound Vib.* **2003**, *262*, 457–474. [[CrossRef](#)]
4. Xu, Z.D.; Xu, Y.S.; Yan, Q.Q.; Xu, C.; Xu, F.H.; Wang, C. Tests and modeling of a new vibration isolation and suppression device. *J. Dyn. Syst. Meas. Control* **2017**, *139*, 121011. [[CrossRef](#)]
5. Mori, K.; Kono, D.; Yamaji, I.; Matsubara, A. Vibration reduction of machine tool using viscoelastic damper support. *Procedia CIRP* **2016**, *46*, 448–451. [[CrossRef](#)]
6. Dai, J.; Xu, Z.D.; Gai, P.P.; Hu, Z.W. Optimal design of tuned mass damper inerter with a Maxwell element for mitigating the vortex-induced vibration in bridges. *Mech. Syst. Signal Process.* **2021**, *148*, 107180. [[CrossRef](#)]
7. Nielsen, E.J.; Lai, M.L.; Soong, T.T.; Kelly, J.M. Viscoelastic damper overview for seismic and wind applications. *Proc. SPIE Smart Mater. Struct.* **1996**, *2720*, 138–144. [[CrossRef](#)]
8. Tsai, C.S.; Lee, H.H. Applications of viscoelastic dampers to high-rise buildings. *J. Struct. Eng.-ASCE* **1993**, *120*, 1222–1233. [[CrossRef](#)]

9. Xu, Z.D. Earthquake mitigation study on viscoelastic dampers for reinforced concrete structures. *J. Vib. Control* **2007**, *13*, 29–45. [[CrossRef](#)]
10. Pant, D.R.; Montgomery, M.; Christopoulos, C. Full-scale testing of a viscoelastic coupling damper for high-rise building applications and comparative evaluation of different numerical models. *J. Struct. Eng.-ASCE* **2018**, *145*, 04018242. [[CrossRef](#)]
11. Xu, Z.D.; Liao, Y.X.; Ge, T.; Xu, C. Experimental and theoretical study on viscoelastic dampers with different matrix rubbers. *J. Eng. Mech. ASCE* **2016**, *142*, 04016051. [[CrossRef](#)]
12. Asano, M.; Masahiko, H.; Yamamoto, M. The experimental study on viscoelastic material dampers and the formulation of analytical model. In Proceedings of the 12th World Conference on Earthquake Engineering, Auckland, New Zealand, 30 January–4 February 2000; p. 1535.
13. Shen, K.L.; Soong, T.T. Modeling of viscoelastic dampers for structural applications. *J. Eng. Mech.-ASCE* **1995**, *121*, 694–701. [[CrossRef](#)]
14. Mazza, F.; Fiore, M.; Mazza, M. Dynamic response of steel framed structures fire-retrofitted with viscoelastic-damped braces. *Int. J. Civ. Eng.* **2017**, *15*, 1187–1201. [[CrossRef](#)]
15. Christopoulos, C.; Montgomery, M. Viscoelastic coupling dampers for enhanced multiple seismic hazard level performance of high-Rise buildings. *Earthq. Spectra* **2018**, *34*, 1847–1867. [[CrossRef](#)]
16. Xu, Z.D.; Shen, Y.P.; Zhao, H.T. A synthetic optimization analysis method on structures with viscoelastic dampers. *Soil Dyn. Earthq. Eng.* **2003**, *23*, 683–689. [[CrossRef](#)]
17. Xu, Z.D.; Zhao, H.T.; Li, A.Q. Optimal analysis and experimental study on structures with viscoelastic dampers. *J. Sound Vib.* **2004**, *273*, 607–618. [[CrossRef](#)]
18. Lakes, R. *Viscoelastic Materials*; Cambridge University Press: New York, NY, USA, 2009.
19. Park, S.W. Analytical modeling of viscoelastic dampers for structural and vibration control. *Int. J. Solids St.* **2001**, *38*, 8065–8092. [[CrossRef](#)]
20. Xu, Y.S.; Xu, Z.D.; Guo, Y.Q.; Ge, T.; Xu, C.; Huang, X.H. Theoretical and experimental study of viscoelastic damper based on fractional derivative approach and micromolecular structures. *J. Vib. Acoust.* **2019**, *141*, 031010. [[CrossRef](#)]
21. Bagley, R.L.; Torvik, P.J. Fractional calculus in the transient analysis of viscoelastically damped structures. *AIAA J.* **1985**, *23*, 918–925. [[CrossRef](#)]
22. Meral, F.C.; Royston, T.J.; Magin, R. Fractional calculus in viscoelasticity: An experimental study. *Commun. Nonlinear Sci.* **2010**, *15*, 939–945. [[CrossRef](#)]
23. Gandhi, F.; Chopra, I. A time-domain non-linear viscoelastic damper model. *Smart Mater. Struct.* **1996**, *5*, 517–528. [[CrossRef](#)]
24. Lewandowski, R. Influence of temperature on the dynamic characteristics of structures with viscoelastic dampers. *J. Struct. Eng.* **2018**, *145*, 04018245. [[CrossRef](#)]
25. Xu, Z.D.; Xu, C.; Hu, J. Equivalent fractional Kelvin model and experimental study on viscoelastic damper. *J. Vib. Control* **2015**, *21*, 2536–2552. [[CrossRef](#)]
26. Cazenove, J.; Rade, D.A.; Lima, A.M.G.D.; Pagnacco, E. A numerical and experimental investigation on self-heating effects in viscoelastic dampers. *Mech. Syst. Signal Process.* **2012**, *27*, 433–445. [[CrossRef](#)]
27. Gopalakrishna, H.S.; Lai, M.L. Finite element heat transfer analysis of viscoelastic damper for wind applications. *J. Wind. Eng. Ind. Aerodyn.* **1998**, *77*, 283–295. [[CrossRef](#)]
28. Lesieutre, G.A.; Govindswamy, K.M. Finite element modeling of frequency-dependent dynamic behavior of viscoelastic materials in simple shear. *Int. J. Solids Struct.* **1995**, *33*, 419–432. [[CrossRef](#)]
29. Schapery, R.A. Effect of cyclic loading on the temperature in viscoelastic media with variable properties. *AIAA J.* **1964**, *2*, 827–835. [[CrossRef](#)]
30. Bérardi, G.; Jaeger, M.; Martin, R.; Carpentier, C. Modelling of a thermo-viscoelastic coupling for large deformations through finite element analysis. *Int. J. Mass Heat Transf.* **1996**, *39*, 3911–3924. [[CrossRef](#)]
31. Drozdov, A.D.; Dorfmann, A. The effect of temperature on the viscoelastic response of rubbery polymers at finite strains. *Acta Mech.* **2002**, *154*, 189–214. [[CrossRef](#)]
32. Inaudi, J.A.; Blondet, M.; Kelly, J.M.; Aprile, A. Heat generation effects on viscoelastic dampers in structures. In Proceedings of the 11th World Conference on Earthquake Engineering, Pergamon Elsevier Science, Oxford, UK, 23–28 June; 28 June 1996; p. 424.
33. Rodas, C.O.; Zaïri, F.; Naït-Abdelaziz, M. A finite strain thermo-viscoelastic constitutive model to describe the self-heating in elastomeric materials during low-cycle fatigue. *J. Mech. Phys. Solids* **2014**, *64*, 396–410. [[CrossRef](#)]
34. Xu, Z.D.; Wang, D.X.; Shi, C.F. Model, tests and application design for viscoelastic dampers. *J. Vib. Control* **2011**, *17*, 1359–1370. [[CrossRef](#)]
35. Deng, Y.J.; Yi, P.Y.; Peng, L.F.; Lai, X.M.; Lin, Z.Q. Flow behavior of polymers during the roll-to-roll hot embossing process. *J. Micromech. Microeng.* **2015**, *25*, 065004. [[CrossRef](#)]
36. Mansour, S.A.; Al-Ghoury, M.E.; Shalaan, E.; El-Eraki, M.H.I.; Abdel-Bary, E.M. Thermal properties of graphite-loaded nitrile rubber/poly (vinyl chloride) blends. *J. Appl. Polym. Sci.* **2010**, *116*, 3171–3177. [[CrossRef](#)]
37. Youssef, H.M.; El-Bary, A.A. Thermal shock problem of a generalized thermoelastic layered composite material with variable thermal conductivity. *Math. Probl. Eng.* **2006**, *2006*, 087940. [[CrossRef](#)]
38. Younis, L.B.; Viskanta, R. Experimental determination of the volumetric heat transfer coefficient between stream of air and ceramic foam. *Int. J. Heat Mass. Transf.* **1993**, *36*, 1425–1434. [[CrossRef](#)]